Sub-3 Å Apoferritin Structures Determined With Single Position Of Volta Phase Plate and the Full Range of Phase Shift

Chen Sun, Kunpeng Li, Thomas Klose, Jose Irimia-Dominguez, Frank S. Vago , Ruben Vidal, Wen Jiang[†]
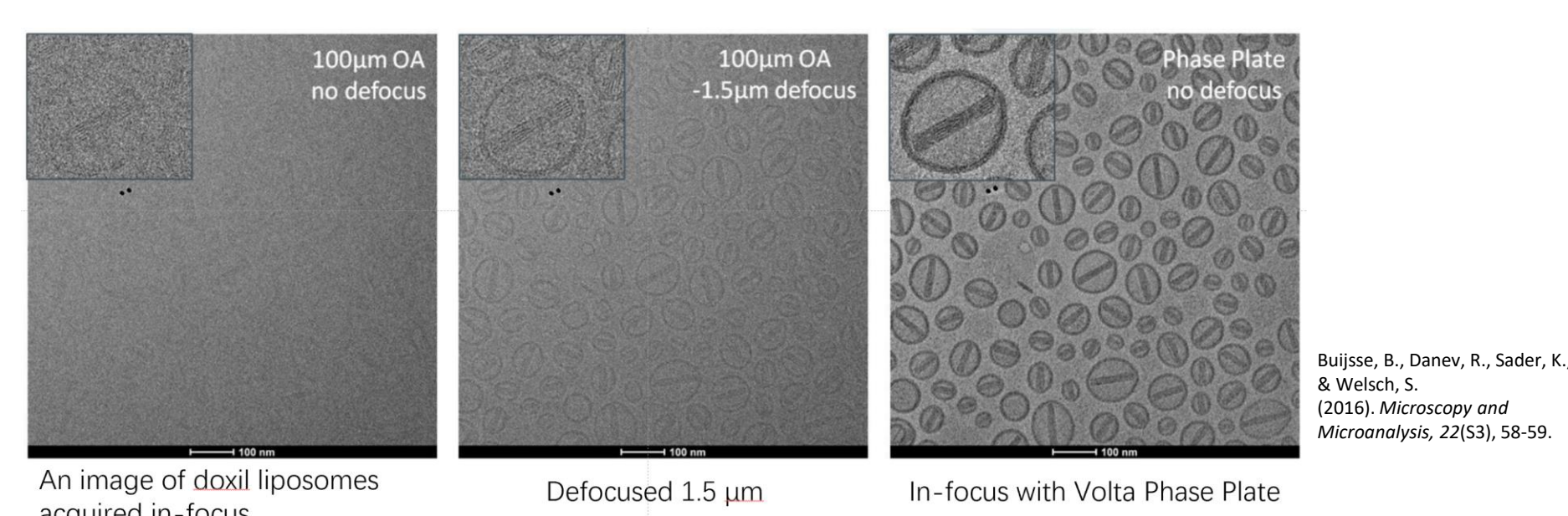
Department of Biological Sciences

jiang12@purdue.edu
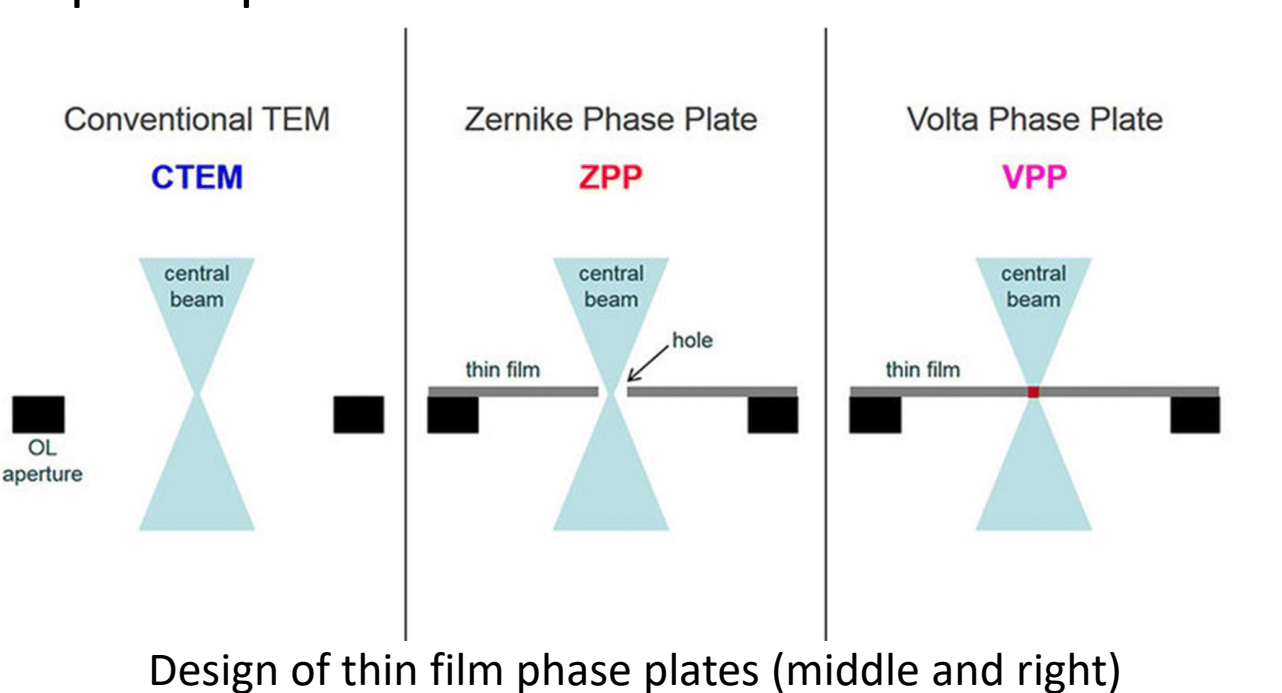
Purdue University, West Lafayette, IN 47907
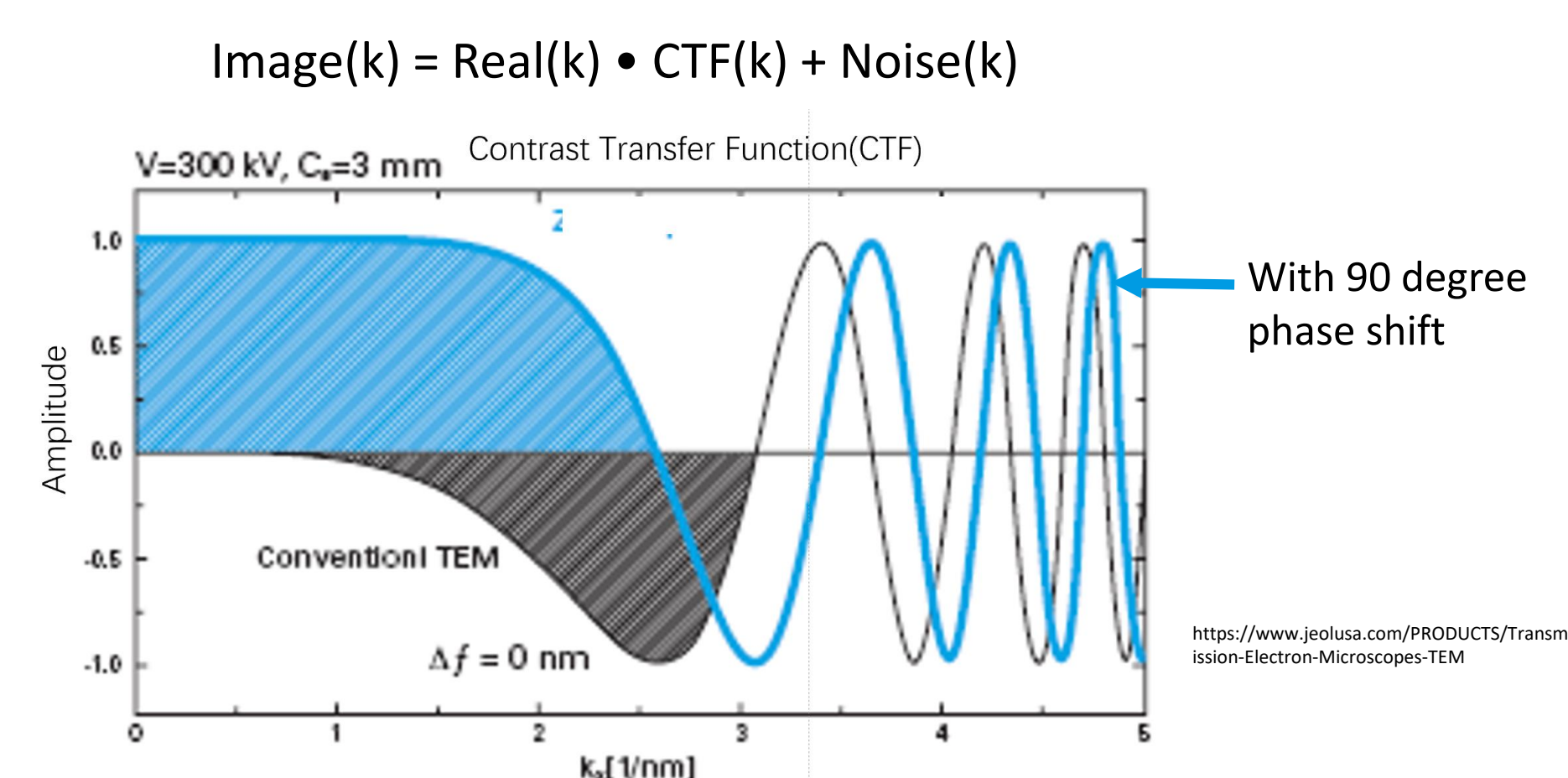
INTRODUCTION

❖ Why do we need phase plate?

An image of doxil liposomes acquired in-focus

Defocused 1.5 µm

In-focus with Volta Phase Plate

Buijsse, B., Danev, R., Sader, K., & Welsch, S. (2016). Microscopy and Microanalysis, 22(S3), 58-59.

❖ What is a phase plate?

Design of thin film phase plates (middle and right)

Radostin Danev, Wolfgang Baumeister, Expanding the boundaries of cryo-EM with phase plates, Current Opinion in Structural Biology

❖ How does a phase plate work?

$$Image(k) = Real(k) \cdot CTF(k) + Noise(k)$$

With 90 degree phase shift

https://www.jeolusa.com/PRODUCTS/Transmission-Electron-Microscopes-TEM
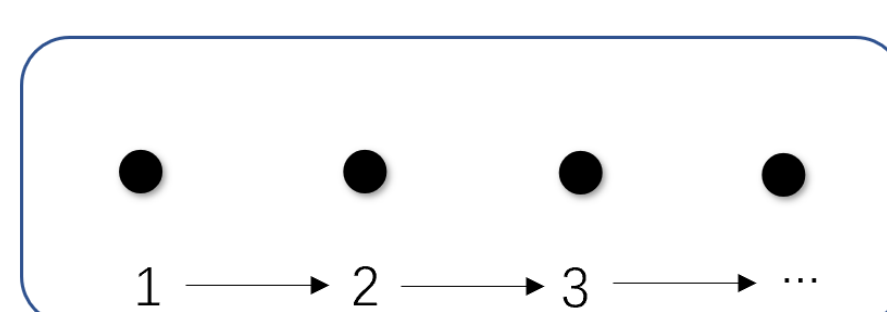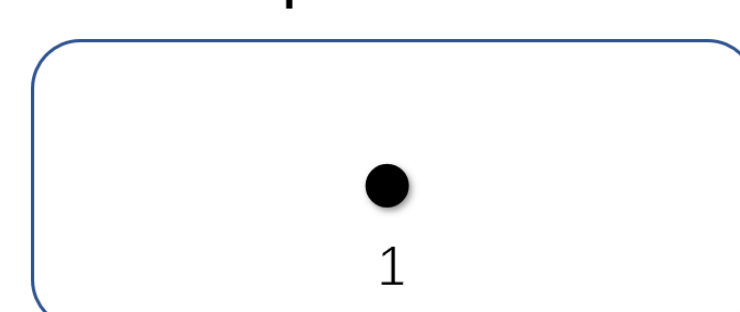
METHOD

Control dataset --Dataset I

VPP position advanced every 30 movies.

Fixed position dataset --Dataset II

The whole dataset was collected with a single VPP position.

Dataset III—a combination of several fixed position datasets
Dataset IV—a large fixed position dataset

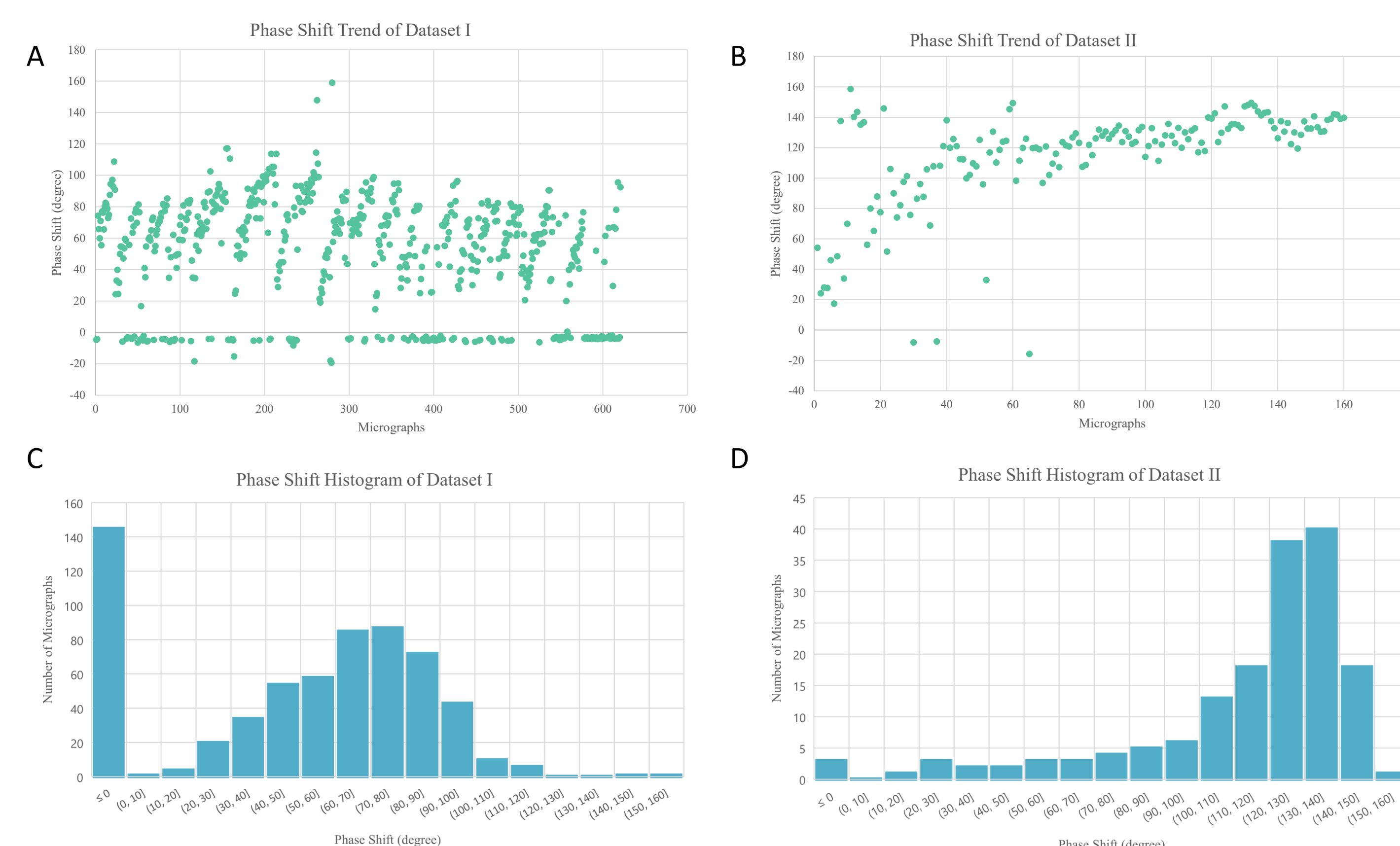|	Dataset I	Dataset II	Dataset III	Dataset IV
Voltage (kV)	300	300	300	300
Dose (e/Å²)	35	35	30	30
Nominal Magnification	22,500	22,500	130,000	130,000
Energy filter	-	-	+	+
VPP age post-installation (months)	6	6	12	14
Number of VPP Positions used	18	1	6	1
Number of Movies	628	160	735	461
Pixel Size (Å)	0.658	0.658	0.535	0.535
Number of frames	50	50	40	40
Resolution (Å)	2.94	2.85	2.51	2.93

RESULTS

Fig. 1. Statistics of phase shifts. (A and B) The time-course of GCTF-determined phase shifts for dataset I (A) and dataset II (B). (C and D) The phase shift distribution of the micrographs of dataset I (C) and dataset II (D).
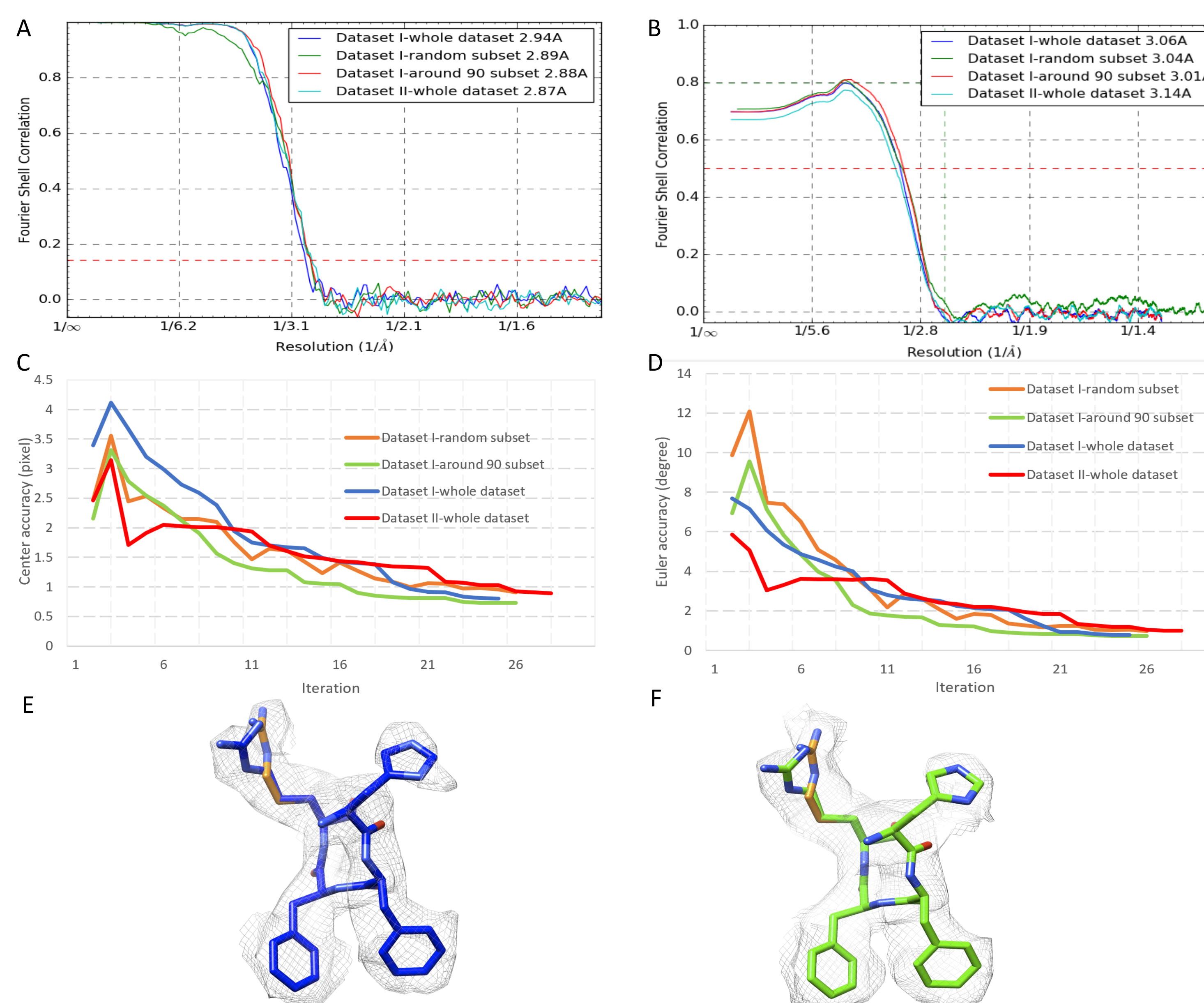

Fig. 2. Comparison of the 3D structures reconstructed from dataset I and dataset II. (A) The Gold Standard FSC curves. (B) The model-map FSC curves of the three maps of dataset I and the map of dataset II. (C and D) The estimated accuracy of center (C) and Euler angles positions (D) in each iteration of 3D refinements. (E and F) Close-up view of the densities and the atomic model of the an alpha-helical segment (a.a. 53–56) for dataset I (E) and dataset II (F).
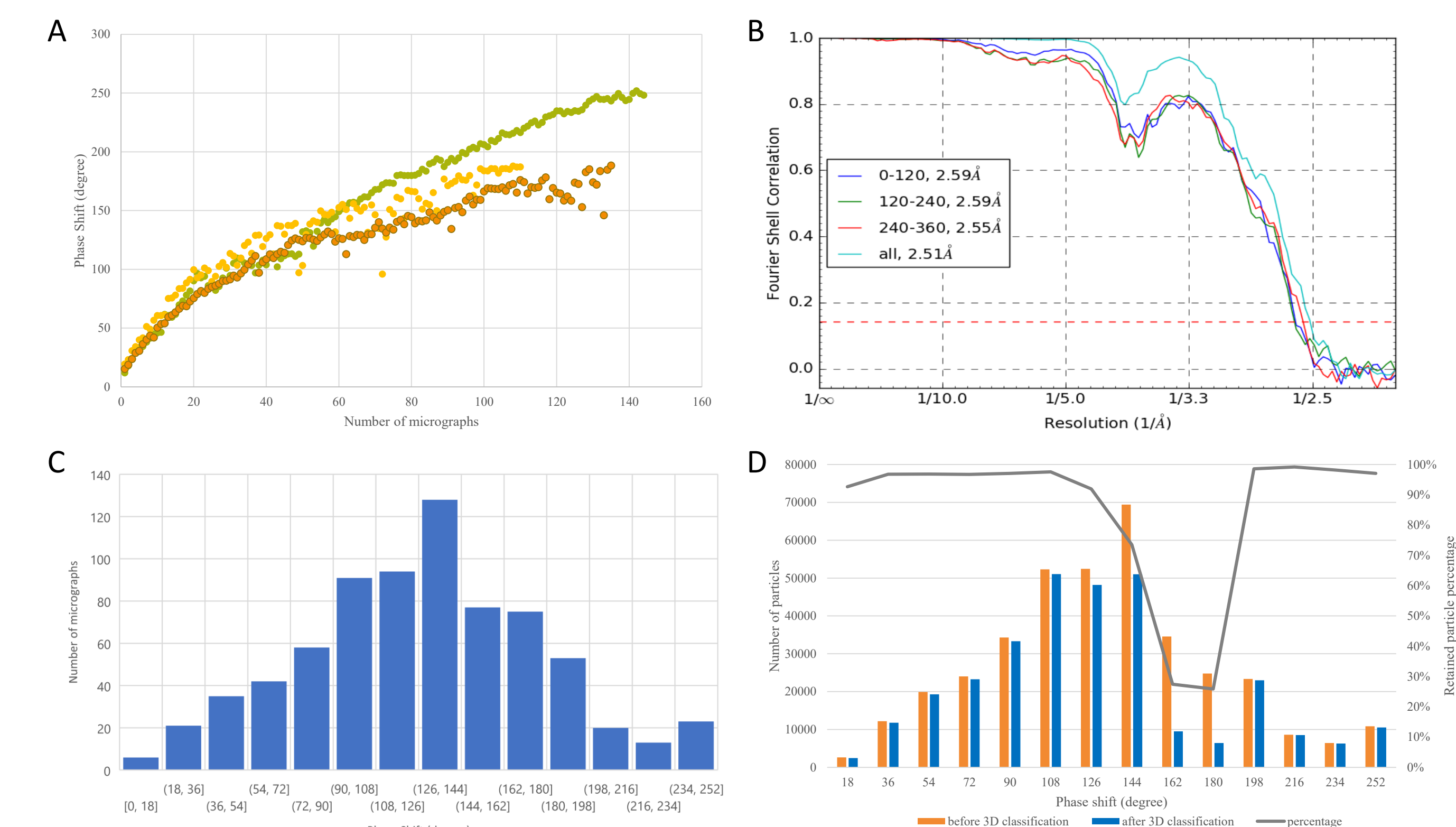

Fig. 3. Image processing results of dataset III. (A) The time-courses of phase shifts of different Volta phase plate spots. (B) The phase shift histogram. (C) The FSC curves. (D) The distribution of the number of particles before and after 3D classification .
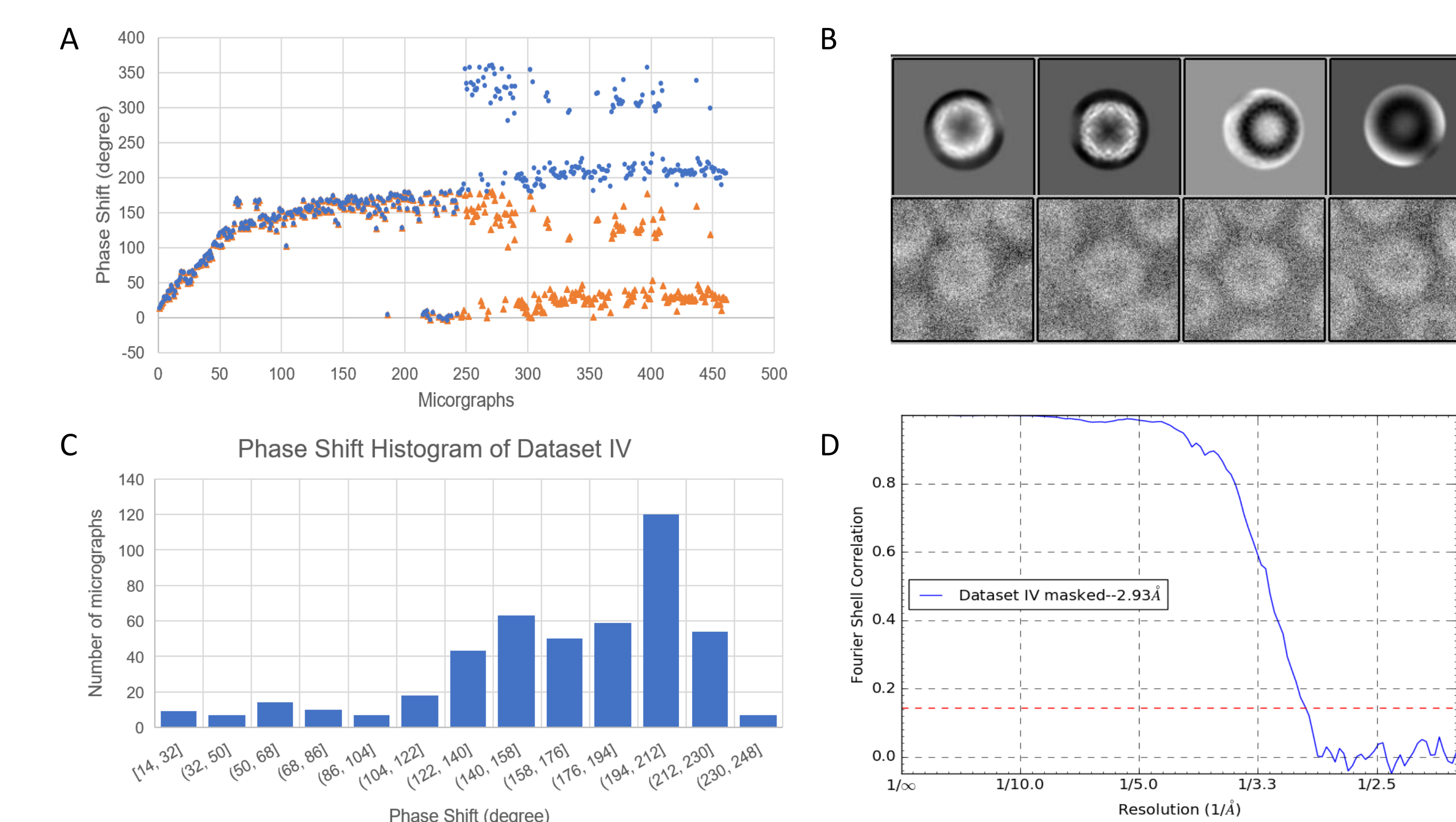

Fig. 4. Image processing results of dataset IV. (A) The time-course of phase shifts determined by *CTFFIND4* (orange triangles) and after manually adding 180 degree to the later micrographs (blue dots). (B) The white and black classes in the 2D classification. (C) The phase shift histogram. (D) The FSC curve for masked half maps.

CONCLUSIONS

➤ A single position of Volta phase plate is able to acquire enough data for high-resolution reconstruction

➤ Particles with phase shifts in the full range have similar quality

➤ Incomplete CTF model for VPP at low resolutions